
Single-Microphone Speaker Separation and Voice Activity Detection in Noisy and Reverberant Environments

Renana Opochnsky¹, Mordehay Moradi¹, and Sharon Gannot¹, Fellow IEEE

¹Bar-Ilan University, Ramat-Gan, 5290002 ISRAEL

Corresponding author: Sharon Gannot (email: sharon.gannot@biu.ac.il).

The project has received funding from the European Union's Horizon 2020 Research and Innovation Programme, Grant Agreement No. 871245; and was also supported by the Israeli Ministry of Science & Technology. Renana Opochnsky and Mordehay Moradi have equally contributed to the paper.

ABSTRACT Speech separation involves extracting an individual speaker's voice from a multi-speaker audio signal. The increasing complexity of real-world environments, where multiple speakers might converse simultaneously, underscores the importance of effective speech separation techniques. This work presents a single-microphone speaker separation network with TF attention aiming at noisy and reverberant environments. We dub this new architecture as Separation TF Attention Network (Sep-TFAnet). In addition, we present a variant of the separation network, dubbed Sep-TFAnet^{VAD}, which incorporates a voice activity detector (VAD) into the separation network.

The separation module is based on a temporal convolutional network (TCN) backbone inspired by the Conv-Tasnet architecture with multiple modifications. Rather than a learned encoder and decoder, we use short-time Fourier transform (STFT) and inverse short-time Fourier transform (iSTFT) for the analysis and synthesis, respectively. Our system is specially developed for human-robotic interactions and should support online mode. The separation capabilities of Sep-TFAnet^{VAD} and Sep-TFAnet were evaluated and extensively analyzed under several acoustic conditions, demonstrating their advantages over competing methods. Since separation networks trained on simulated data tend to perform poorly on real recordings, we also demonstrate the ability of the proposed scheme to better generalize to realistic examples recorded in our acoustic lab by a humanoid robot. Project page: <https://Sep-TFAnet.github.io>

INDEX TERMS speaker separation, voice activity detection, temporal convolutional networks.

I. Introduction

BLIND speaker separation is a rapidly growing research field aiming to separate a mixture of speech signals into their components. This technology has important applications in robot audition, speech recognition, hearing aids, and telecommunications. The introduction of deep clustering (DC) [1] and permutation invariant training (PIT) [2] has sparked increasing interest in single-microphone speaker separation algorithms that rely on deep neural networks (DNNs).

Many recent separation schemes are directly applied in the time domain using learnable encoder-decoder structure, e.g., Conv-Tasnet [3], dual-path recurrent neural network (DPRNN) [4] and many more [5]–[8].

The Conv-Tasnet algorithm, as introduced in [3], employs one-dimensional convolutional layers to infer self-learned representations of the input signal. These embedded-domain representations are utilized to compute masks for each individual speaker, which are subsequently applied to separate the speakers. This approach employs the scale-invariant signal-to-distortion ratio (SI-SDR) [9] loss function, specifically designed to capitalize on temporal information. The algorithm achieves improved performance compared with state-of-the-art (SOTA) methods, probably because its features are learned rather than manually designed.

A transformer-based neural network architecture, dubbed SepFormer, was presented [10] and [11]. The successive downsampling and resampling of multi-resolution features (SuDoRmRf), presented in [12], is based on simple one-

dimensional convolution layers requiring significantly less memory and parameters than the existing aforementioned methods. Several challenges and limitations remain unsolved in current methods. Many of them perform poorly in the presence of background noise and high reverberation, resulting in significant degradation in the quality of the separated signals. Robustness to noise and reverberation is a key challenge in real-world applications of speech source separation. These approaches mainly focused on a non-realistic anechoic dataset as WSJ-2mix [1] and WHAM! [13]. Specifically, the frame length is relatively short in time domain approaches, allowing proper separation only in an anechoic environment [14], [15].

In the current contribution, we propose the Sep-TFAnet, a modified separation approach that leverages the Conv-Tasnet [3] backbone, using TCN, toward a more realistic scenario. By incorporating an attention layer and training with reverberant references, the proposed network improves the separation scores in more challenging environments compared to other competing methods. In addition, we propose Sep-TFAnet^{VAD}, which simultaneously infers all speakers’ activity patterns. In other words, together with the separation, we jointly train a VAD network. VAD is an essential component in multiple downstream tasks, e.g., post-filters, beamforming, and localization. Note that several papers combine VAD with multi-channel speech processing [16], [17], and for extraction [17].

One of the main objectives of Sep-TFAnet^{VAD} is to improve a robot’s auditory capabilities. Developing socially assistive robots that can perform multi-person interactions requires progress in speech-related tasks such as speech source separation, localization, etc. The robot is supposed to function in a crowded environment. Therefore, we trained and adapted our system to complex acoustic conditions. In this context, the VAD can be utilized as a voice activity controller, assisting the robot in engaging in human-like interactions. The VAD decisions can facilitate applying a post-filtering operation to suppress further residual interfering signals and noise and enable the estimation of several building blocks of subsequent multichannel processing, e.g., an linearly constrained minimum variance (LCMV) beamformer.

In the proposed network, inspired by Conv-Tasnet [3], we substitute the learnable time domain encoder-decoder with an STFT to better deal with high reverberation scenarios. In [14], it was demonstrated that the STFT is a more valid choice for the encoder and decoder stages than the learnable representations. It is also demonstrated that jointly addressing both reverberation and overlapped speech appears to be a challenging task.

Furthermore, this paper introduces a new simulated dataset with more realistic conditions, such as the typical overlap between speakers and higher perceived reverberation level than the WHAMR! dataset [18]. Moreover, we also introduce real-world data recorded on a humanoid robot. Our model

performs comparably or better than SOTA models on this new, more challenging dataset.

The main contributions of this paper are: 1) A more realistic dataset including “real-world” experiments; 2) An elaborate network based on Tasnet that outperforms SOTA methods in challenging scenarios; 3) An ‘online mode’ for low latency applications in practical setups; 4) An extensive analysis of the separation results; and 5) A VAD that operates in parallel to the separation module and achieves accurate activity readings.

The paper is organized as follows. In Sec. II, we formulate the separation problem. In Sec. III, we describe the proposed model, Sep-TFAnet, and its components. In Sec. IV, we demonstrate the performance of the proposed algorithm through an extensive simulation study and real-world recordings. A comparison between the Sep-TFAnet (with and without VAD) and the competing algorithms is carried out. Section V concludes the paper.

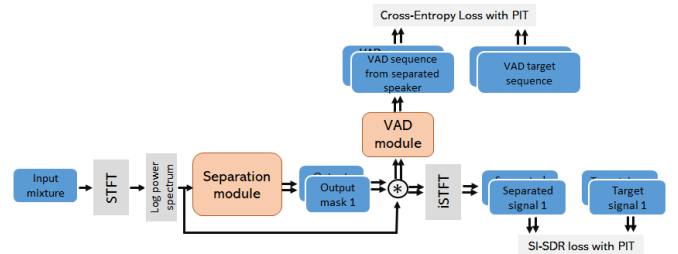


FIGURE 1: Sep-TFAnet^{VAD} architecture. Learnable blocks are depicted in orange, and data blocks are in blue.

II. Problem Formulation

Let $x(t)$ be a mixture of I concurrent speakers captured by a single microphone:

$$x(t) = \sum_{i=1}^I \{s_i * h_i\}(t) + n(t) \quad t = 0, 1, \dots, T - 1, \quad (1)$$

where $s_i(t)$ represents the signal of the i -th speaker, $h_i(t)$ represents the, possibly time-varying, room impulse response (RIR) between the i -th speaker and the microphone, and $n(t)$ represents an additive noise. Time variations of the RIR can be attributed to either the sources’ movements, the microphone, or both. In this paper, we deal with static scenarios. In the STFT domain, and under the assumption of sufficiently long time frames, (1) can be reformulated as,

$$x(l, k) = \sum_{i=1}^I s_i(l, k)h_i(l, k) + n(l, k), \quad (2)$$

where $l \in \{0, \dots, L - 1\}$ and $k \in \{0, \dots, K - 1\}$ are the time-frame and the frequency-bin indexes, respectively, with L the total number of time-frames and K the total number of frequency bins. In our study, we only address the case $I = 2$. Denote the outputs of the separator system in the STFT domain as $\hat{s}_1(l, k)$ and $\hat{s}_2(l, k)$.

We assume a fully-supervised setting, in which the goal is to infer a model that separates two output signals $\hat{s}_1(t)$ and $\hat{s}_2(t)$ from an unseen mixture $x(t)$, by maximizing the SI-SDR between the separated signals and the reverberated clean signals, $\{s_1 * h_1\}(t)$ and $\{s_2 * h_2\}(t)$, respectively.

In addition, in one version of our system Sep-TFAnet^{VAD}, the activity of each separated speaker per time frame is determined by applying a VAD network. This task also assumes a fully-supervised training.

III. Proposed Model

The model comprises two main components: a separation module and a VAD module. The separation module is based on a temporal convolutional network (TCN) backbone [19]. Rather than a learned encoder and decoder, we use the STFT and the iSTFT. As demonstrated in [14], [20], audio processing algorithms that are based on STFT-iSTFT are advantageous in high reverberation as compared with learned encoder-decoder.

The VAD module determines the activity patterns of each separated signal and can be useful in downstream tasks. A block diagram of the entire system is depicted in Fig. 1.

Next, we elaborate on the various components of the system.

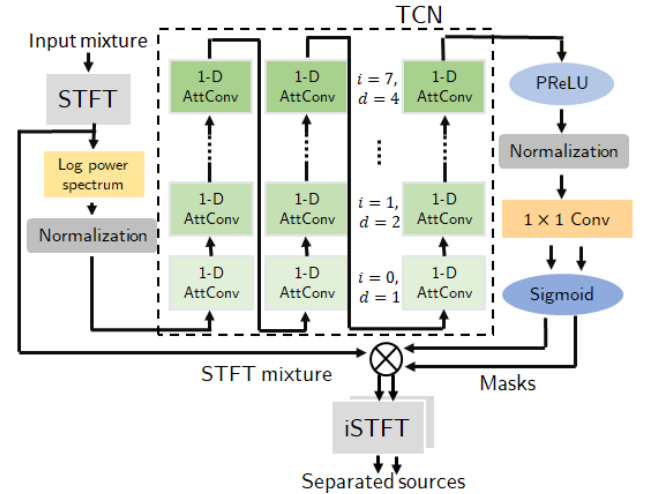
A. Separation Module

The Separation Module is the main component of our proposed scheme. The various components of this module are depicted in Fig. 2.

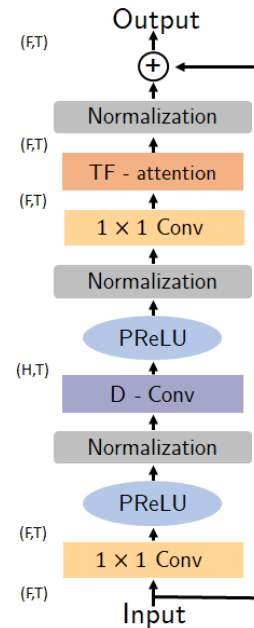
An STFT first analyzes the raw audio signal. Then, the log-spectrum is calculated, followed by layer normalization (LN). The result of these operations constitutes the input to the separation network. The main processing module is an adapted TCN (dashed part in Fig. 2a). Originally, the TCN is a series of identical 1-D Conv blocks with increasing dilation factors and with zero-padding along the time dimension to maintain their integrity. The dilation factor enables capturing a sufficiently long temporal context of the speech signal. We stress that past STFT frames are also relevant for the separation task in high reverberation levels and should be considered. Here, the adapted TCN consists of three repeats of a stack of eight 1-D AttConv blocks, as proposed in [3] and depicted in Figs. 2a, 2b.

Unlike the original 1-D Conv blocks in the Conv-Tasnet algorithm [3], our 1-D AttConv blocks have only one output and do not feature an additional skip connection output from the output of each block to the overall TCN output (see Fig. 2b). We have decided to avoid this additional output since according to empirical evidence indicated in [21] and affirmed by our findings, they do not improve performance but rather increase the number of parameters.

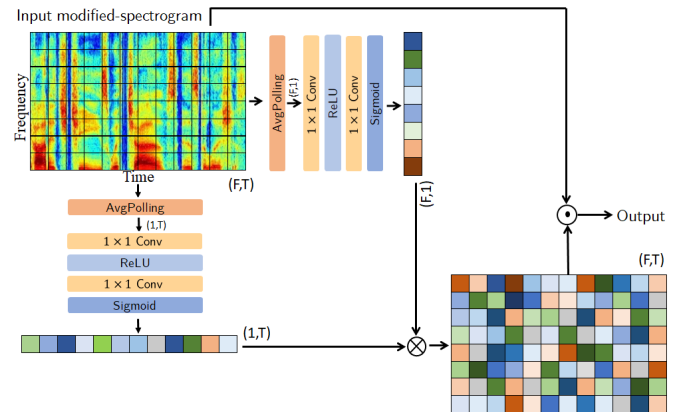
For each 1-D AttConv block (see Fig. 2b), the input of the block is summed to its output. Additionally, since the input to our network is an STFT representation, the dilation factors were chosen to maintain as small as possible receptive field



(a) Separation module



(b) 1-D AttConv



(c) TF attention layer

FIGURE 2: Separation Module: Architecture.

but long enough to address reverberation. As a suitable compromise, we set $d = (i \bmod 4) + 1$, $0 \leq i \leq 7$, where d is the dilation factor and i denotes the number of the 1-D AttConv block in each repeat as depicted in Fig. 2a. The first 1×1 Conv layer in each 1-D AttConv block has a kernel size 1. The number of filters is set to F , the number of frequency bins, to capture the frame-wise frequency patterns. In addition, following the 1×1 Conv layer, the D-Conv layer expounded upon in [3], is subsequently applied with H output filters, $H > F$ with the purpose of achieving a richer representation while concurrently minimizing the number of parameters.

Another component contributing to the network’s performance is the time-frequency (TF) attention block adopted from [22], which was proposed in the context of noise reduction. The TF attention block is depicted in Fig. 2c. This block is positioned after the final 1×1 Conv layer of each 1-D AttConv block, followed by a normalization layer, to optimize further the network’s ability to learn to recognize complex patterns in speech data. Despite its relatively small number of parameters, this module improves the performance by approximately 0.5 dB. As depicted in Fig. 2c, the block commences with average pooling layers on both the time and frequency dimensions, followed by 1×1 Conv layers and activation functions. These layers generate an attention mask, subsequently multiplied element-wise with the modified spectrogram of the input signal.

Finally, after applying all 1-D AttConv blocks, a pre-exponential linear unit (PReLU) activation function, along with a LN and a 1×1 Conv, is employed to estimate the masks, which are subsequently passed through a Sigmoid activation function, which output is confined to the interval $[0, 1]$ as depicted in Fig. 2. In conjunction with the STFT, this activation function preserves the audio scale of the output along the utterance and can be beneficial in online mode. The estimated speakers’ signals are transformed back to the time domain by augmenting the masked spectrum with the noisy and mixed input signal phase and then applying the iSTFT.

B. Online Mode

Developing an online variant of the separation algorithm is vital in human-robot communication, as it may facilitate proper interaction between the robot and the human speaker. We employ a distinctive strategy instead of processing the complete utterance in batch mode. We divide the input into short segments comprising past, present, and future samples. We apply the separation operation to each segment by employing a sliding window. To maintain consistency of the separated signals between all segments, we apply PIT with $L1$ loss. Notably, the step size for the aforementioned sliding window technique is set to be equal to the number of future samples.

C. Voice activity detector (VAD) network

The purpose of the VAD network is to infer the activity patterns of the separated speakers. The inputs to the network are the extracted masks from the jointly trained separation module. The VAD network consists of a 1-D convolution layer with four filters, followed by a PReLU activation function and a normalization layer. The activity patterns of the corresponding speakers are finally obtained by applying a 1-D convolutional layer with one filter, followed by a hard threshold to obtain a binary activity decision for each frame. In addition, we modify the 1-D AttConv block, as proposed in [23], such that the output of 1-D AttConv block is:

$$\text{output}^{\text{1-D AttConv}} = \text{LN}(x + \text{LN}(x + y_{\text{att}})) \quad (3)$$

where x is the input to the AttConv block, and y_{att} is the output of the TF-attention layer within the AttConv block.

D. Objective Functions

We experimented with several separation objective functions to efficiently train the model and found that the SI-SDR loss yields the best perceptual improvement. The loss is formulated as follows:

$$\text{SI-SDR}(s, \hat{s}) = 10 \log_{10} \left(\frac{\left\| \frac{\langle \hat{s}, s \rangle}{\langle s, s \rangle} s \right\|^2}{\left\| \frac{\langle \hat{s}, s \rangle}{\langle s, s \rangle} s - \hat{s} \right\|^2} \right). \quad (4)$$

To alleviate the permutation problem, common to separation problems, utterance-level permutation invariant training (uPIT) [24] was employed. We stress that the target signals during training were the reverberant signals, namely the anechoic signals convolved with the corresponding RIRs. Hence, the signal focuses on the separation task and does not attempt to dereverberate the separated signals. While this may improve separation scores, the performance of automatic speech recognition (ASR) systems may deteriorate in high reverberation levels. If reverberation is an issue, a dereverberation module, e.g., [25] or [26], can be applied as a post-filter.

For training the VAD module, we have used the binary cross entropy (BCE) loss:

$$\text{BCE} = - \sum_{i=1}^I \sum_{l=0}^{L-1} v_i(l) \log(p_i(l)) + (1 - v_i(l)) \log(1 - p_i(l)), \quad (5)$$

where $p_i(l)$ is the output of the VAD network indicating the probability of speaker $i = 1, \dots, I$ at time frame l to be active, $v_i(l)$ is the true activity of speaker i at time frame l .

IV. Experimental Study

A. Datasets

The WHAMR! dataset [18] is widely used for speech separation in reverberant environments. According to our tests, the reported reverberation level, $0.1 - 1$ s, is inaccurate, and in practice, it is perceived as less reverberant than

reported.¹ We have, therefore, constructed our own database with another simulator and used it for training and evaluation in conjunction with the WHAMR! dataset.

To generate our dataset, clean speech utterances were drawn from the clean corpus of the Librispeech database [27] and then convolved with RIRs generated using the image method [28] implemented in [29]. The reverberation level is uniformly set in the [0.2, 0.6] s range. The reverberated signals were then mixed with SIR=0 dB and contaminated with babble noise from the WHAMR! dataset [13] with SNR uniformly drawn in the range [0, 15] dB. The speakers were located in random positions (under physical constraints) inside shoebox rooms with random dimensions. The room’s length and width were uniformly drawn in the range [4.5, 6.5] m, and the room’s height was uniformly drawn in the range [2.5, 3] m. The speakers are partially overlapping, with overlap percentage randomly selected from [50%, 75%, 100%]. The length of each sample is 10 Sec. Overall, our simulated data consists of 155 hours of audio samples for train, 39 hours for validation, and 22 hours for testing.

B. Robot Interaction: Experimental Setup

To further analyze the algorithm’s performance in a real-world setting, specifically in the context of robot audition, a recording campaign was held in the acoustic laboratory at Bar-Ilan University. This lab is a $6 \times 6 \times 2.4$ m room with a reverberation time controlled by 60 interchangeable panels covering the room facets. In our experiments, the reverberation time was set (by changing the panel arrangements) to either 350 ms, typical of a meeting room, or 600 ms, typical of a lecture hall. The room layout is depicted in Fig. 3a.

ARI² by PAL Robotics is a humanoid robot with an Intel i9 processor and Nvidia Orin GPU. The goal of our project is to improve the social capabilities of the robot and specifically to develop its capabilities to engage with patients in a hospital environment.³

ARI is equipped with ReSpeaker 4-Microphone Array v2.0,⁴ installed inside the robot’s compartment, 80 cm above its base. We only used one of the microphones for evaluating the single-microphone algorithms.

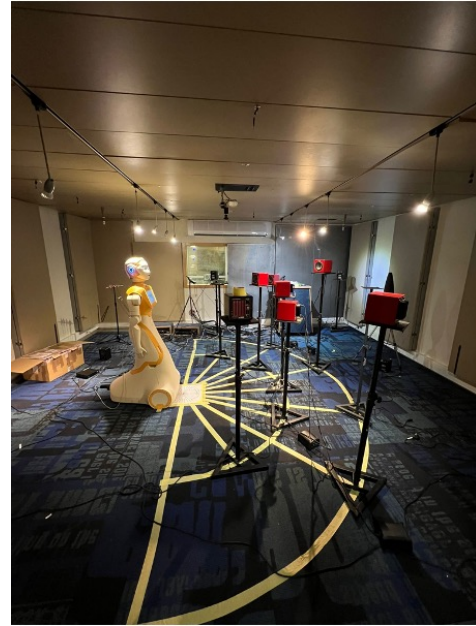
In our experimental setup, ARI was positioned at the center of the acoustic lab, with a set of loudspeakers in front of it, on two semi-circles with approximately 1 m and 2 m radius, respectively. Our experiments only used the inner semi-circle with five loudspeakers positioned at $[-65, -30, 0, 30, 65]^\circ$. To generate a sample, we randomly selected two loudspeakers and played speech utterances randomly drawn from the Librispeech test set [27]. The utterances were separately recorded by ARI and then manually

¹Analyzing the WHAMR! recipe for Pyroomacoustics, we believe that this discrepancy results in from the definition of the reflection coefficient.

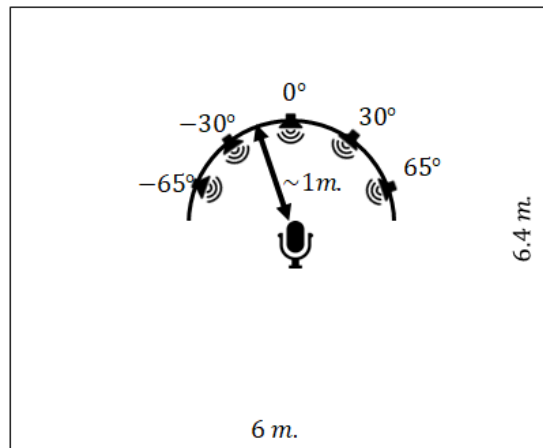
²<https://pal-robotics.com/robots/ari/>

³SPRING - Socially Pertinent Robots in Gerontological Healthcare, a project under the Horizon2020 programme, <https://spring-h2020.eu/>.

⁴https://wiki.seeedstudio.com/ReSpeaker_Mic_Array_v2.0/



(a) Recording setup with ARI at BIU acoustic lab. ARI was positioned at the center of the acoustic lab, with a set of loudspeakers in front of it, on two semi-circles with approximately 1 m and 2 m radius, respectively. In our experiments, we only used the inner semi-circle with five loudspeakers positioned at $[-65, -30, 0, 30, 65]^\circ$. The speech signals were simultaneously played from two randomly chosen loudspeakers. The lab’s computer automatically controlled the entire scenario.



(b) Geometric setup of the experiment at BIU Acoustic Lab.

FIGURE 3: Experimental setup with ARI robot in the center of the Bar-Ilan acoustic lab with loudspeakers in a semi-circle at the front of the robot.

mixed to enable SI-SDR calculation. The overlap between the speakers was randomly set in the range $[25\%, 50\%]$. No external noise was added to the recordings; hence, only sensor and low-level ambient noise are present. Overall, 200 samples were generated at each reverberation level. The experimental setup is schematically depicted in Fig. 3b.

C. Training Procedure

In this section, we give the technical details of the training procedure. The model was trained on GPU servers, Tesla V100 SXM2 32GB, using 315 epochs. A $1e^{-3}$ learning rate was chosen, coupled with the Adam optimizer. During the training process, gradient clipping is applied with a maximum L2-norm of 5 to ensure stability and prevent exploding gradients. The model has approximately 5M trainable parameters. The parameters of the STFT and hyperparameters of the network are detailed in Table 1.

TABLE 1: The parameters of the STFT and hyperparameters of Sep-TFAnet^{VAD}.

| | Variable | Value |
|----------------|---------------|---------|
| STFT | Hop length | 256 |
| | FFT bins | 512 |
| | Window | Hamming |
| | Window length | 512 |
| Hyperparameter | H | 512 |
| | F | 256 |
| | F_s | 16 kHz |
| | Batch size | 16 |

D. Baseline Methods

We compared the proposed method to two competing methods that have a comparable number of parameters, the SuDoRmRf [12], [30] and the Conv-Tasnet [3]. SuDoRmRf model leverages the effectiveness of iterative temporal resampling strategies to avoid the need for multiple stacked dilated convolutional layers. Another baseline method is the Conv-Tasnet algorithm [3], as it shares a similar backbone with our separation module, namely the TCN module. The Conv-Tasnet is applied in the time domain with learned encoder-masking-decoder architecture. As mentioned previously, our approach diverges from the original Conv-Tasnet method in several important aspects. The Conv-Tasnet and our networks have a similar number of parameters ~ 5.5 million, while the SuDoRmRf model is more compact with ~ 2.7 million parameters. We trained the baselines with our new simulated dataset for the results reported in the current paper.

E. Experimental Results

1) Separation with Simulated Data

The SI-SDR, averaged over all utterances, for Sep-TFAnet, Sep-TFAnet^{VAD} and competing algorithms for both the WHAMR! database and the new simulated data are depicted

in Table 2. The SI-SDR scores of the proposed method and

TABLE 2: Averaged SI-SDR [dB]

| Algorithm | WHAMR! | Simulated Data |
|---------------------------|------------|----------------|
| Unprocessed (mix) | -0.86 | -2.04 |
| Sep-TFAnet | 8.1 | 6.92 |
| Sep-TFAnet ^{VAD} | 7.86 | 6.77 |
| SuDoRmRf | 7.04 | 5.6 |
| Conv-Tasnet | 8.3 | 6.6 |

the Conv-Tasnet are comparable, while the SuDoRmRf performance is lower. It is also evident that the new simulated data is more challenging than the WHAMR! database.

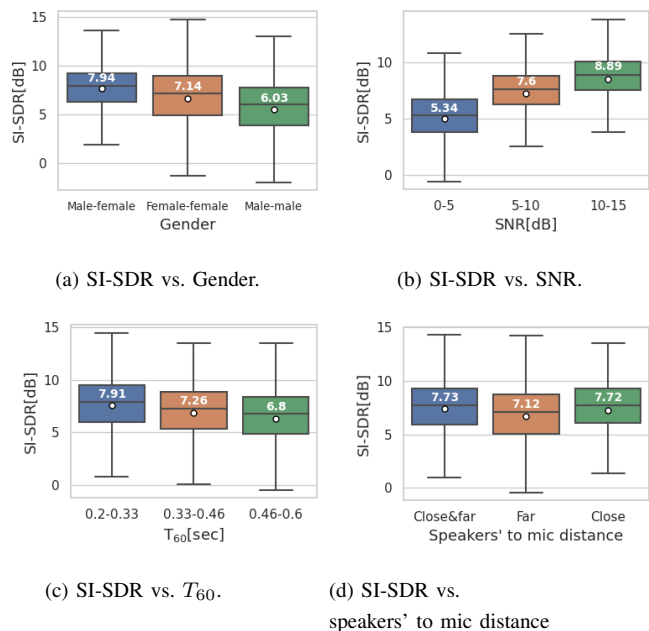
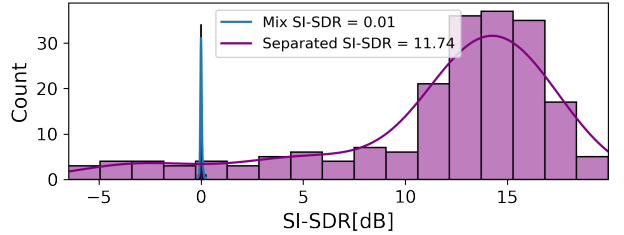


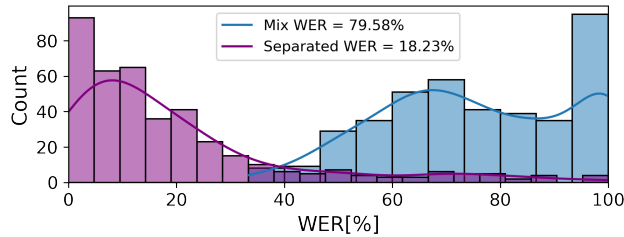
FIGURE 4: The SI-SDR of the proposed algorithm tested on our new simulated dataset and categorized according to speakers' gender, signal-to-noise ratio (SNR) level, reverberation level, and speakers-to-mic distance. The number indicates the median value, while the mean score is indicated by \circ .

Further insights into the performance of Sep-TFAnet can be inferred by carefully examining the statistics of the results. Figure 4 depicts box plots of the SI-SDR categorized according to speakers' gender, SNR level, reverberation level, and speakers' to-mic distance. It is evident from Fig. 4a that the best results are obtained for the mixed-gender case, while the worst results are for the male-male mixture. A marginal improvement is demonstrated with increasing SNR level, as evident from Fig. 4b. The dependency on the reverberation level is indicated in Fig. 4c, with a clear performance drop from lower levels to higher levels of T_{60} . Finally, as depicted in Fig. 4d, best results are obtained if

the distance of both sources from the microphone is lower than the critical distance (and consequently high direct-to-reverberation ratio (DRR)), and worst when both sources are beyond the critical distance. It should be stressed that above the critical distance, the reverberation tail dominates the RIR, and hence, the signal is perceived as more reverberant.



(a) SI-SDR histograms



(b) word error rate (WER) histograms

FIGURE 5: SI-SDR and WER improvements with ARI recordings, $T_{60} = 0.35$ s and low sensor noise. The overlap of the speakers was randomly set to the range [25%, 50%].

2) Separation with Data Recorded on ARI Robot

We have also used the database recorded on the robot’s microphone to verify the algorithm’s applicability to our scenarios. In the network’s regular mode, a significant improvement both in terms of WER (using NVIDIA RIVA Conformer-based ASR⁵) and SI-SDR can be deduced from the histograms in Fig. 5, analyzing the results for $T_{60} = 0.35$ sec and low-sensor noise scenario. The mean SI-SDR was improved from approximately 0 dB to 11.74 dB, and the mean WER from 76% to 18.23%.

Table 3 depicts the mean SI-SDR and WER results of this real-world experiments for the proposed algorithm (with and without VAD), and Conv-Tasnet. We present the results for the regular mode (batch processing). The online mode will be discussed in the next section.

In the $T_{60} = 0.35$ sec case, it is evident that the proposed algorithm significantly outperforms the Conv-Tasnet and achieves much lower WER. The performance advantages are less pronounced for the $T_{60} = 0.6$ sec case, with our proposed algorithm only slightly outperforming Conv-Tasnet. We also note that Sep-TFAnet performs better than Sep-TFAnet^{VAD} in both T_{60} conditions. For qualitative

⁵https://catalog.ngc.nvidia.com/orgs/nvidia/teams/tao/models/speechtotext_en_us_conformer

TABLE 3: Mean separation results on ARI recorded data.

| Mode | Algorithm | SI-SDR[dB] | | WER | |
|---------|---------------------------|----------------|-------------|--------------|--------------|
| | | T_{60} [sec] | | | |
| | | 0.35 | 0.6 | 0.35 | 0.6 |
| Regular | Sep-TFAnet | 11.74 | 9 | 18.23 | 24.96 |
| | Sep-TFAnet ^{VAD} | 11.55 | 8.7 | 18.69 | 26.41 |
| | Conv-Tasnet | 10.88 | 8.33 | 27.6 | 27.71 |
| Online | Sep-TFAnet | 11.64 | 8.4 | 18.3 | 26.51 |
| | Sep-TFAnet ^{VAD} | 9.87 | 7.81 | 23.88 | 29.77 |
| | Conv-Tasnet | 9.88 | 8.31 | 21.32 | 26.16 |

assessment, we give examples of separated signals with sonograms and transcriptions in Fig. 6. The reverberation level was chosen as $T_{60} = 0.35$ sec with 50% overlap between the speakers’ activities. The loudspeakers were located at 35° and 60° . In this example, the output SI-SDR was 12.11[dB] and the WER 15.3% while Conv-Tasnet only achieved 4.2[dB] and 43.75%, respectively.

3) Online Mode

To facilitate low-latency implementation, we applied the algorithm to 3 sec long segments with a 1 sec look-ahead. The results for online mode are depicted in the lower part of Table 3, indicating only a slight degradation compared to batch mode.

4) Analysis of VAD Results

The VAD results were compared to a simple energy-based VAD and to WebRTC VAD network. In the energy-based VAD, each T-F bin at the output of the separation network (the mask) is compared with an activation threshold and classified as an active or non-active bin. For each time frame, if the number of active bins exceeds a threshold, the frame is declared a speech-active frame. We examined several threshold pairs and selected the most suitable pair based on the best VAD accuracy. We used $T_a = 0.3$ and $T_s = 0.25$, where T_a is the T-F bin activation threshold and T_s is the threshold for the number of bins to declare speech-active frame. WebRTC⁶ is a project providing real-time communication capabilities for many different applications. The VAD implemented in WebRTC is reportedly one of the best VADs available. In setting this VAD, we used a latency of 30 ms and multiple frequency band features with a pre-trained GMM classifier. Using the new simulated dataset, our embedded VAD achieved accuracy, recall, and precision measures of 94%, 0.96%, 0.94%, the energy-based VAD achieved 73%, 0.96%, 0.73%, and the WebRTC VAD achieved 84%, 0.99%, 0.8%, respectively. We can, therefore, conclude that incorporating the VAD into the separation scheme is beneficial in terms of detection accuracy, although

⁶Available online at <https://webrtc.org/>

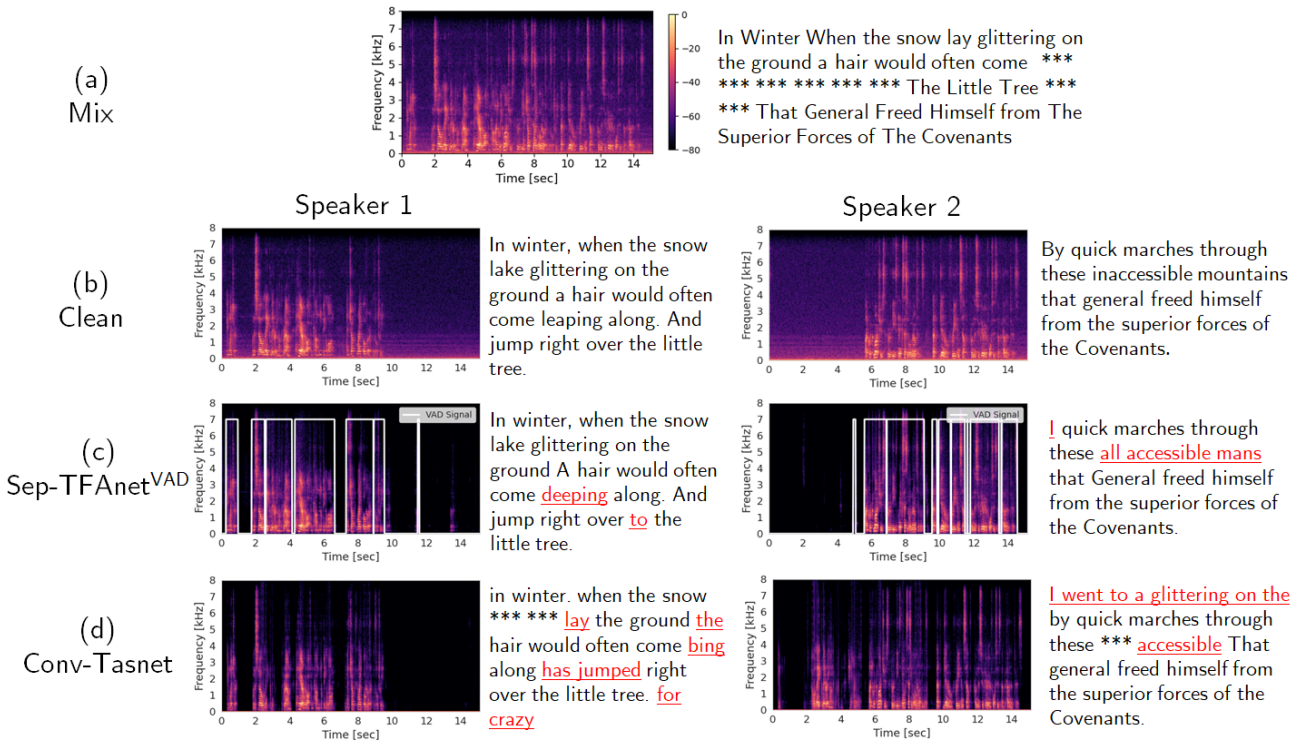


FIGURE 6: Spectrograms of (a) mixed-signal, (b) clean-reference signals, (c) separated outputs of our network, VAD outputs in white on our results, (d) separated outputs of Tasnet and respective transcripts. The words in red indicate wrong transcription, and ‘*’ - indicates missing words. The reverberation level was $T_{60} = 0.35$ sec with 50% overlap between the speakers. The loudspeakers were located at 35° and 60° .

it comes with a slight performance degradation in the speaker separation measures.

V. Conclusions

We presented a speaker separation algorithm that employs a TCN module. Our results indicate that our model performs comparably or better than current state-of-the-art separation methods, with the added benefits of success in real-world scenarios. A comprehensive experimental study with both simulated and real recordings supports our claims. Furthermore, we have demonstrated the effectiveness of using the STFT-iSTFT instead of the learnable encoder and decoder as in [14]. This approach, which leverages the compact STFT representation, proves advantageous in minimizing memory consumption. It should be noted that selecting an adequately large window size is crucial to ensure stable performance in the presence of reverberation.

A new simulated dataset incorporating more realistic adverse acoustic conditions was also introduced. We also comprehensively analyzed the results, considering various parameters such as speakers’ gender, signal-to-noise ratio (SNR) level, reverberation level, and distance between the speakers and the microphone. The method was also applied to real-world data recorded on a humanoid robot in our acoustic laboratory at BIU. By applying our method to this dataset, we demonstrate its superior performance compared

to competing methods in a challenging and realistic scenario in both SI-SDR and WER measures. Our separation algorithm was tested with NVIDIA’s ASR system and significantly improved the WER in mid-level reverberation, $T_{60} \approx 350$ ms, and low noise levels. The overlap between speakers was set in a realistic range, imitating normal conversations, as fully overlapping utterances are unrealistic.

We note that in the current audio processing architecture, two independent audio streams are simultaneously transcribed by the ASR system. For later use by the dialogue system, we may also use our VAD decisions to preserve the time consistency of the transcribed speech signals. The VAD can also prove beneficial in applying a subsequent processing stage, e.g., multi-microphone beamforming. The embedded VAD outperforms both naïve and state-of-the-art VADs.

Acknowledgments

We thank Mr. Pini Tandeitnik and Mr. Yoav Elinson for their professional assistance during the acoustic room setup, the recordings, and the ASR application. We also thank Yoav Elinson for thoroughly analyzing the reverberation level in the WHAMR! dataset signals.

REFERENCES

[1] J. R. Hershey, Z. Chen, J. Le Roux, and S. Watanabe, “Deep clustering: Discriminative embeddings for segmentation and separation,” in *IEEE international conference on acoustics, speech and signal processing (ICASSP)*, pp. 31–35, 2016.

- [2] D. Yu, M. Kolbæk, Z.-H. Tan, and J. Jensen, "Permutation invariant training of deep models for speaker-independent multi-talker speech separation," in *IEEE International Conference on Acoustics, Speech and Signal Processing (ICASSP)*, pp. 241–245, 2017.
- [3] Y. Luo and N. Mesgarani, "Conv-tasnet: Surpassing ideal time-frequency magnitude masking for speech separation," *IEEE/ACM transactions on audio, speech, and language processing*, vol. 27, no. 8, pp. 1256–1266, 2019.
- [4] Y. Luo, Z. Chen, and T. Yoshioka, "Dual-path RNN: efficient long sequence modeling for time-domain single-channel speech separation," in *IEEE International Conference on Acoustics, Speech and Signal Processing (ICASSP)*, pp. 46–50, 2020.
- [5] N. Zeghidour and D. Grangier, "Wavesplit: End-to-end speech separation by speaker clustering," *IEEE/ACM Transactions on Audio, Speech, and Language Processing*, vol. 29, pp. 2840–2849, 2021.
- [6] S. Zhao and B. Ma, "Mossformer: Pushing the performance limit of monaural speech separation using gated single-head transformer with convolution-augmented joint self-attentions," in *IEEE International Conference on Acoustics, Speech and Signal Processing (ICASSP)*, 2023.
- [7] E. Nachmani, Y. Adi, and L. Wolf, "Voice separation with an unknown number of multiple speakers," in *International Conference on Machine Learning (ICML)*, pp. 7164–7175, 2020.
- [8] S. Lutati, E. Nachmani, and L. Wolf, "SepIt approaching a single channel speech separation bound," *arXiv preprint arXiv:2205.11801*, 2022.
- [9] J. Le Roux, S. Wisdom, H. Erdogan, and J. R. Hershey, "SDR—half-baked or well done?," in *IEEE International Conference on Acoustics, Speech and Signal Processing (ICASSP)*, pp. 626–630, 2019.
- [10] C. Subakan, M. Ravanelli, S. Cornell, M. Bronzi, and J. Zhong, "Attention is all you need in speech separation," in *IEEE International Conference on Acoustics, Speech and Signal Processing (ICASSP)*, pp. 21–25, 2021.
- [11] C. Subakan, M. Ravanelli, S. Cornell, F. Grondin, and M. Bronzi, "On using transformers for speech-separation," *arXiv preprint arXiv:2202.02884*, 2022.
- [12] E. Tzinis, Z. Wang, X. Jiang, and P. Smaragdus, "Compute and memory efficient universal sound source separation," *Journal of Signal Processing Systems*, vol. 94, no. 2, pp. 245–259, 2022.
- [13] G. Wichern, J. Antognini, M. Flynn, L. R. Zhu, E. McQuinn, D. Crow, E. Manilow, and J. L. Roux, "WHAM!: Extending Speech Separation to Noisy Environments," in *Proc. Interspeech*, pp. 1368–1372, 2019.
- [14] T. Cord-Landwehr, C. Boeddeker, T. Von Neumann, C. Zorilă, R. Dod-dipatla, and R. Haeb-Umbach, "Monaural source separation: From anechoic to reverberant environments," in *International Workshop on Acoustic Signal Enhancement (IWAENC)*, 2022.
- [15] J. Heitkaemper, D. Jakobeit, C. Boeddeker, L. Drude, and R. Haeb-Umbach, "Demystifying TasNet: A dissecting approach," in *IEEE International Conference on Acoustics, Speech and Signal Processing (ICASSP)*, pp. 6359–6363, 2020.
- [16] D. Wang, T. Yoshioka, Z. Chen, X. Wang, T. Zhou, and Z. Meng, "Continuous speech separation with ad hoc microphone arrays," in *2021 29th European Signal Processing Conference (EUSIPCO)*, pp. 1100–1104, IEEE, 2021.
- [17] Q. Lin, L. Yang, X. Wang, L. Xie, C. Jia, and J. Wang, "Sparsely overlapped speech training in the time domain: Joint learning of target speech separation and personal vad benefits," in *2021 Asia-Pacific Signal and Information Processing Association Annual Summit and Conference (APSIPA ASC)*, pp. 689–693, IEEE, 2021.
- [18] M. Maciejewski, G. Wichern, E. McQuinn, and J. Le Roux, "WHAMR!: Noisy and reverberant single-channel speech separation," in *IEEE International Conference on Acoustics, Speech and Signal Processing (ICASSP)*, pp. 696–700, 2020.
- [19] C. Lea, R. Vidal, A. Reiter, and G. D. Hager, "Temporal convolutional networks: A unified approach to action segmentation," in *European Conference on Computer Vision (ECCV)*, (Amsterdam, The Netherlands), pp. 47–54, Springer, Oct. 2016.
- [20] Z.-Q. Wang, G. Wichern, S. Watanabe, and J. Le Roux, "STFT-domain neural speech enhancement with very low algorithmic latency," *IEEE/ACM Transactions on Audio, Speech, and Language Processing*, vol. 31, pp. 397–410, 2022.
- [21] W. Ravenscroft, S. Goetze, and T. Hain, "Deformable temporal convolutional networks for monaural noisy reverberant speech separation," in *IEEE International Conference on Acoustics, Speech and Signal Processing (ICASSP)*, 2023.
- [22] Q. Zhang, X. Qian, Z. Ni, A. Nicolson, E. Ambikairajah, and H. Li, "A time-frequency attention module for neural speech enhancement," *IEEE/ACM Transactions on Audio, Speech, and Language Processing*, vol. 31, pp. 462–475, 2023.
- [23] F. Liu, X. Ren, Z. Zhang, X. Sun, and Y. Zou, "Rethinking skip connection with layer normalization," in *Proceedings of the 28th international conference on computational linguistics*, pp. 3586–3598, 2020.
- [24] M. Kolbæk, D. Yu, Z.-H. Tan, and J. Jensen, "Multitalker speech separation with utterance-level permutation invariant training of deep recurrent neural networks," *IEEE/ACM Transactions on Audio, Speech, and Language Processing*, vol. 25, no. 10, pp. 1901–1913, 2017.
- [25] Y. Yemini, E. Fetaya, H. Maron, and S. Gannot, "Scene-agnostic multi-microphone speech dereverberation," in *Proc. of Interspeech*, (Brno, The Czech Republic), 2021.
- [26] M. Delcroix, T. Yoshioka, A. Ogawa, Y. Kubo, M. Fujimoto, N. Ito, K. Kinoshita, M. Espi, T. Hori, T. Nakatani, *et al.*, "Linear prediction-based dereverberation with advanced speech enhancement and recognition technologies for the reverb challenge," in *Reverb workshop*, 2014.
- [27] V. Panayotov, G. Chen, D. Povey, and S. Khudanpur, "Librispeech: an asr corpus based on public domain audio books," in *IEEE International Conference on Acoustics, Speech and Signal Processing (ICASSP)*, pp. 5206–5210, 2015.
- [28] J. B. Allen and D. A. Berkley, "Image method for efficiently simulating small-room acoustics," *The Journal of the Acoustical Society of America*, vol. 65, no. 4, pp. 943–950, 1979.
- [29] E. A. Habets, "Room impulse response generator," tech. rep., Friedrich-Alexander-Universität Erlangen-Nürnberg, 2014.
- [30] E. Tzinis, Z. Wang, and P. Smaragdus, "Sudo rm-rf: Efficient networks for universal audio source separation," in *IEEE International Workshop on Machine Learning for Signal Processing (MLSP)*, 2020.